Steel and Composite Structures, *Vol. 16, No. 2 (2014) 203-220*
DOI: http://dx.doi.org/10.12989/scs.2014.16.2.203

Numerical analysis of interface crack problem in composite plates jointed with composite patch

Fatih Cetisli [*1] and Mete O. Kaman [2b]

[1] *Department of Civil Engineering, Pamukkale University, Denizli 20070, Republic of Turkey*
[2] *Department of Mechanical Engineering, Firat University, Elazig 23119, Republic of Turkey*

(*Received July 05, 2012, Revised September 30, 2013, Accepted October 24, 2013*)

Abstract. Stress intensity factors are numerically investigated for interfacial edge crack between two dissimilar composite plates jointed with single side composite patch. Variation of stress intensity factor under Mode I loading condition is examined for different material models and fiber orientation angles of composite plates and patch. ANSYS 12.1 finite element analysis software is used to obtain displacements of crack surfaces in the numerical solution and repaired plates are modeled in three dimensions. Obtained results are presented in the form of graphs. It is found that fiber orientation angle of composites is an effective parameter on interfacial stress intensity factor.

Keywords: interface crack; composite patch; stress intensity factor; finite element method

1. Introduction

The fiber composite materials are taking over the place of traditional materials to decrease the weight of air, land, and sea vehicles. Adhesives are commonly preferred at joints of fiber composites that are used in construction of these vehicles, in which the lightness, rigidity, and reliability are important. Since geometrical discontinuities occur in mechanical joints due to the joint holes, loss of strength in plates due to the stress condensation is observed. This brings the adhesive joints, in which uniform stress distribution is observed, to the front when compared to the demountable joints.

Although there are various types of adhesive joints depending on the status of the parts to be jointed, single lap and double lap joint types are preferred commonly. Variations in joint types designate the strength of the joint so that the reliability of the construction. In addition to numerical studies (Apalak 2006, Her 1999, Sheppard *et al*. 1998) on stress and damage analysis, which are conducted by using Finite Element Method (FEM) for different adhesion parameters, experimental studies (Abdelaziz *et al*. 2006, Atas *et al*. 2011, Temiz 2006, Zhang *et al*. 2010) also showed that the variations in joint types, humidity, temperature, and adhesive thickness vitally affect the strength of the joint.

Adhesive joints are used also in repair of defects on composite materials beside the joint of

*Corresponding author, Assistant Professor, Ph.D., E-mail: fcetisli@pau.edu.tr
[a] Associate Professor, E-mail: mkaman@firat.edu.tr

http://www.techno-press.org/?journal=scs&subpage=8 ISSN: 1229-9367 (Print), 1598-6233 (Online)

composite materials. The easy applicability of single lap joint and patch, which is the reason to be preferred, provided achieving successful results, especially in repair of cracks on the body and inner surface of planes, by using composite patches (Belhouari *et al*. 2004).

With the developments in FEM besides the experimental studies (Jones and Chiu 1999, Schubbe and Mall 1999, Seo and Lee 2002), which were conducted to understand the effect of patch and to obtain ideal repair design, the number of numerical studies increased. Oudad *et al*. (2009) investigated the performance of metallic structures that are repaired with fiber composite patches by using 3D nonlinear FEM. It was mentioned by Oudad *et al*. (2009) that the size of the plastic region at crack tip is remarkably reduced with the use of composite patch. The performance of circular composite patch for single and double lap repair on plates with central crack was investigated with using a 3D FEM by Albedah *et al*. (2011). It was found by Albedah *et al*. (2011) that double sided patches decrease the stress intensity factor and circular patches provide mass gain. The mechanical behavior of A17075-76 material with a V-shape notch that is repaired with 1 and 4 layers of composite patches was studied by Gu *et al*. (2011) by using FEM. The contour integral method was used to investigate the effect of layer layout besides the material and thickness of adhesive epoxy and patch on stress intensity factor by Gu *et al*. (2011). It was noted by Gu *et al*. (2011) that shear strength and adhesive thickness are the major factors on performance of the patch. Bezzerrouki *et al*. (2008) compared the stress intensity factor of aluminum plates with edge crack that are repaired with double-side patch with single layer adhesive and single-side patch with double layers of adhesive by using FEM. Bezzerrouki *et al*. (2008) found that increasing the shear strength in double-side patch and decreasing the thickness of adhesive while increasing the patch thickness in single-side patch bring advantage in repair of edge cracks on aluminum plates.

The literature is concentrated on repair of aluminum alloys that are widely used in aerospace industry. However, with the recent technologic developments the use of composite materials is spread out so that the analyses of cracks at adhesive joints gained importance. The most effective damages in composite plates that are jointed with adhesive are the cracks in between plates and interfacial crack in between the adhesive and the plate. The analyses of interface cracks in composite plates gain importance at this point. The asymptotic solution for interface crack problem in anisotropic material was studied by Hwu (1993). The FEM was used by Sun and Qian (1997) to solve the interface crack problem in orthotropic materials. Ikeda *et al*. (2006) calculated the SIF for interface cracks in dissimilar anisotropic materials by using the formulations of Stroh (1962). The energy release rates under plain strain conditions were calculated by using virtual crack extension method thru FEM. The presented method accurately provided mode-separated stress intensity factors using relatively coarse meshes for the finite element method. The SIF for 3D interfacial cracks in dissimilar anisotropic materials were calculated with M-integral method by Nagai *et al*. (2007a, b). Excellent agreement was achieved between the numerical results obtained by the presented method and the corresponding results proposed by other researchers. Rogel and Sills (2010) examined delamination between two layers of a fiber-reinforced composite material oriented in the directions θ / (θ-90°). The behavior of the stress and displacement fields near the crack tip was studied. In order to calculate the stress intensity factors, a three-dimensional interaction energy or conservative M-integral was extended and implemented in conjunction with the finite element method. The displacement extrapolation method was also extended for this case. Sills and Ikeda (2011) investigated stress intensity factors for interface cracks between orthotropic and monoclinic material. Two different expressions used in the literature for the stress intensity factors of interface cracks was discussed and compared for orthotropic and monoclinic materials.

Hemant *et al*. (2005) obtained strain energy release rate components for an interface crack in two-dimensional orthotropic media using the finite element analysis. The individual and total strain energy release rates were calculated using the modified crack closure integral method. Nagai *et al*. (2007a, b) applied the virtual crack extension method and the thermal M-integral method for a crack along the interface between two different materials to the thermoelastic interfacial crack in anisotropic bimaterials. The moving least-squares approximation was used to calculate the value of the thermal M-integral.

It was shown by various studies (Belhouari *et al*. 2004, Bezzerrouki *et al*. 2008, Bouiadjra *et al*. 2007, Madani *et al*. 2008) that the characteristics of the adhesive and especially the composite patch are effective on the stress intensity factor. The fiber orientation angle of continuous fiber reinforced composites plays a vital role in mechanical behavior of the material.

The interfacial stress intensity factor of composite plates that are jointed with adhesive, have an edge crack, and repaired with composite patch on single side are numerically investigated. The effect of the fiber orientation angle in plates and composite patches on stress intensity factor is investigated by using a 3D finite element model for various composite materials. The numerical analysis is conducted with ANSYS 12.1 finite element analysis software. The stress intensity factor at crack tip of the composite plate is calculated by using displacement extrapolation method. The obtained results are presented with graphs.

2. Material and method

2.1 Stress intensity factor of interface crack between dissimilar orthotropic materials

Firstly, stress intensity factor of interfacial edge crack are examined for two dissimilar orthotropic plate having arbitrary fiber orientations. Hwu (1993) defined the stress intensity factors of an interface crack between dissimilar anisotropic materials.

$$\begin{Bmatrix} K_{II} \\ K_{I} \\ K_{III} \end{Bmatrix} = \lim_{r\to 0} \sqrt{2\pi r}\,\Lambda \left\langle\!\!\left\langle \left(\frac{r}{l_k}\right)^{-i\varepsilon_\alpha} \right\rangle\!\!\right\rangle \Lambda^{-1} \begin{Bmatrix} \sigma_{12} \\ \sigma_{22} \\ \sigma_{32} \end{Bmatrix} \tag{1}$$

where r is distance from crack tip, l_k is an arbitrary characteristic length, ε_α (α = 1, 2, 3) involve the bimaterial constant, $\langle\langle\ \rangle\rangle$ denote a diagonal matrix, $i = \sqrt{-1}$. Matrix Λ is composed of three eigenvectors

$$\Lambda = [\lambda_1, \lambda_2, \lambda_3] \tag{2}$$

of the following eigenvalue problem

$$(M^* + e^{2i\pi\delta}\overline{M}^*)\lambda = 0 \tag{3}$$

where δ_α (α = 1, 2, 3) are eigenvalues which are given by Ting (1986) as the explicit solution

$$\delta_\alpha = -\frac{1}{2} + i\varepsilon_\alpha\,, \quad (\alpha = 1, 2, 3) \tag{4}$$

$$\varepsilon_1 = \varepsilon = \frac{1}{2\pi}\ln\frac{1+\beta}{1-\beta},\quad \varepsilon_2 = -\varepsilon,\quad \varepsilon_3 = 0 \tag{5}$$

$$\beta = \left[-\frac{1}{2}tr(WD^{-1})^2\right]^{\frac{1}{2}} \tag{6}$$

where *tr* stands for the trace of a matrix; ε is called the oscillation index. M^* is a bimaterial matrix

$$M^* = D - iW \tag{7}$$

obtained from the Barnett-Lothe tensors (Barnett and Lothe 1973) of two materials

$$D = L_1^{-1} + L_2^{-1} \tag{8}$$

$$W = S_1^* L_1^{-1} - S_2^* L_2^{-1} \tag{9}$$

Here, the subscripts 1 and 2 denote upper and lower materials, respectively (Fig. 1).

For orthotropic materials, the matrices S^* and L are expressed in the following form (Liou and Sung 2008)

$$S^* = \begin{bmatrix} 0 & -Y_{12}Y_{22}^{-1} & 0 \\ Y_{12}Y_{11}^{-1} & 0 & 0 \\ 0 & 0 & 0 \end{bmatrix} \tag{10.a}$$

$$L = \begin{bmatrix} Y_{11}^{-1} & 0 & 0 \\ 0 & Y_{22}^{-1} & 0 \\ 0 & 0 & Y_{33}^{-1} \end{bmatrix} \tag{10.b}$$

where

$$Y_{11} = \frac{-iC_{22}(C_{12}+C_{66})(\mu_1+\mu_2)}{C_{66}(C_{22}\mu_1^2 - C_{12})(C_{22}\mu_2^2 - C_{12})} \tag{11.a}$$

$$Y_{22} = \frac{-iC_{22}(C_{12}+C_{66})(\mu_1+\mu_2)(\mu_1\mu_2)}{C_{66}(C_{22}\mu_1^2 - C_{12})(C_{22}\mu_2^2 - C_{12})} \tag{11.b}$$

$$Y_{12} = \frac{-(C_{12}+C_{66})(C_{22}\mu_1\mu_2 + C_{12})}{C_{66}(C_{22}\mu_1^2 - C_{12})(C_{22}\mu_2^2 - C_{12})} \tag{11.c}$$

$$Y_{33} = (C_{44}C_{55})^{-1/2} \tag{11.d}$$

The C_{ij} (i, j = 1,…,6) is the stiffness coefficients of the material and the μ_i, (i = 1,…,3) in Eq.

(11) are the positive roots of imaginary parts of the compatibility equation.

$$l_2(\mu)l_4(\mu)-[l_3(\mu)]^2=0 \tag{12}$$

where

$$l_2(\mu)=M_{55}\mu^2-2M_{45}\mu+M_{44} \tag{13.a}$$

$$l_3(\mu)=M_{15}\mu^3-(M_{14}+M_{16})\mu^2+(M_{25}+M_{46})\mu-M_{24} \tag{13.b}$$

$$l_4(\mu)=M_{11}\mu^4-2M_{16}\mu^3+(2M_{12}+M_{66})\mu^2-2M_{26}\mu+M_{22} \tag{13.c}$$

and in case of plane strain

$$M_{ij}=S_{ij}-\frac{S_{i3}-S_{j3}}{S_{33}}\ ,\ \ (i,j=1,\ldots,6) \tag{14}$$

The S_{ij} $(i, j = 1,\ldots,6)$ is the compliance coefficients of the material ($[C]=[S]^{-1}$). The stress-strain relationship for orthotropic material is given in Eq. (15).

$$\begin{Bmatrix}\varepsilon_1\\ \varepsilon_2\\ \varepsilon_3\\ \varepsilon_4\\ \varepsilon_5\\ \varepsilon_6\end{Bmatrix}=\begin{bmatrix}S_{11} & S_{12} & S_{13} & 0 & 0 & 0\\ S_{12} & S_{22} & S_{23} & 0 & 0 & 0\\ S_{13} & S_{23} & S_{33} & 0 & 0 & 0\\ 0 & 0 & 0 & S_{44} & 0 & 0\\ 0 & 0 & 0 & 0 & S_{55} & 0\\ 0 & 0 & 0 & 0 & 0 & S_{66}\end{bmatrix}\begin{Bmatrix}\sigma_1\\ \sigma_2\\ \sigma_3\\ \sigma_4\\ \sigma_5\\ \sigma_6\end{Bmatrix}=\begin{bmatrix}\frac{1}{E_1} & -\frac{v_{21}}{E_2} & -\frac{v_{31}}{E_3} & 0 & 0 & 0\\ -\frac{v_{12}}{E_1} & \frac{1}{E_2} & -\frac{v_{32}}{E_3} & 0 & 0 & 0\\ -\frac{v_{13}}{E_1} & -\frac{v_{23}}{E_2} & \frac{1}{E_3} & 0 & 0 & 0\\ 0 & 0 & 0 & \frac{1}{G_{23}} & 0 & 0\\ 0 & 0 & 0 & 0 & \frac{1}{G_{13}} & 0\\ 0 & 0 & 0 & 0 & 0 & \frac{1}{G_{12}}\end{bmatrix}\begin{Bmatrix}\sigma_1\\ \sigma_2\\ \sigma_3\\ \sigma_4\\ \sigma_5\\ \sigma_6\end{Bmatrix} \tag{15}$$

It is noted that for orthotropic materials the two roots μ_1 and μ_2 in Eq. (16.c) have a relation in between as

$$\mu_1\mu_2=-(C_{11}/C_{22})^{1/2} \tag{16.a}$$

$$\mu_1^2+\mu_2^2=-\frac{C_{11}C_{22}-C_{12}(C_{12}+2C_{66})}{C_{22}C_{66}} \tag{16.b}$$

$$\mu_1+\mu_2=i\left[\frac{C_{11}C_{22}-C_{12}(C_{12}+2C_{66})}{C_{22}C_{66}}+2\left(\frac{C_{11}}{C_{22}}\right)^{1/2}\right]^{1/2} \tag{16.c}$$

In this case, [*S**] and [*L*] can be rewritten as

$$S^* = \begin{bmatrix} 0 & S_{12}^* & 0 \\ S_{21}^* & 0 & 0 \\ 0 & 0 & 0 \end{bmatrix} = \begin{bmatrix} 0 & -\sqrt{(C_{22}/C_{11})}S_{21}^* & 0 \\ \sqrt{\dfrac{C_{66}(\sqrt{C_{11}C_{22}}-C_{12})}{C_{22}(C_{12}+2C_{66}+\sqrt{C_{11}C_{22}}}} & 0 & 0 \\ 0 & 0 & 0 \end{bmatrix} \tag{17.a}$$

$$L = \begin{bmatrix} L_{11} & 0 & 0 \\ 0 & L_{22} & 0 \\ 0 & 0 & L_{33} \end{bmatrix} = \begin{bmatrix} (C_{12}+\sqrt{C_{11}+C_{22}})S_{21}^* & 0 & 0 \\ 0 & \sqrt{(C_{22}/C_{11})}L_{11} & 0 \\ 0 & 0 & \sqrt{C_{44}C_{55}} \end{bmatrix} \tag{17.b}$$

If the fibers in a composite plate are rotated as θ_1 and θ_2 degrees from the x-axis (Fig. 1), the modified Barnett-Lothe tensors can be obtained by using (Dongye and Ting 1989, Qian and Sun 1998)

$$S^*(\theta) = \Omega(\theta) S^* \Omega^T(\theta) \tag{18a}$$

$$L(\theta) = \Omega(\theta) L \Omega^T(\theta) \tag{18b}$$

where

$$\Omega(\theta) = \begin{bmatrix} \cos(\theta) & \sin(\theta) & 0 \\ -\sin(\theta) & \cos(\theta) & 0 \\ 0 & 0 & 0 \end{bmatrix} \tag{19}$$

If Eqs. (17.a)-(17.b) are put into the Eqs. (8)-(9), the D and W matrices can be obtained by using Eqs. (18.a)-(18.b) in the following form

$$D = L_1^{-1} + L_2^{-1} = \begin{bmatrix} D_{11} & D_{12} & 0 \\ D_{12} & D_{22} & 0 \\ 0 & 0 & 0 \end{bmatrix} \tag{20}$$

$$W = S_1^* L_1^{-1} - S_2^* L_2^{-1} = \begin{bmatrix} 0 & -W_{21} & 0 \\ W_{21} & 0 & 0 \\ 0 & 0 & 0 \end{bmatrix} \tag{21}$$

In here, coefficients of the [D] and [W] matrices are

$$D_{11} = \sum_{i=1}^{2} \frac{L_{11}^i \sin^2\theta_i + L_{22}^i \cos^2\theta_i}{L_{11}^i L_{22}^i} \tag{22.a}$$

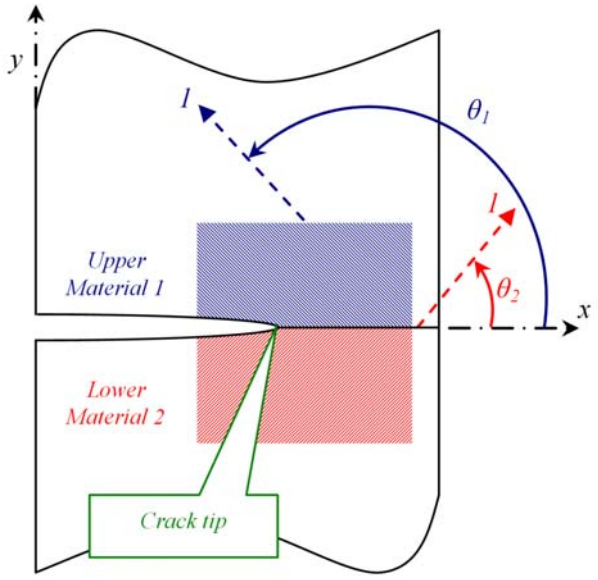

Fig. 1 Interfacial edge crack between two dissimilar orthotropic materials

$$D_{11} = \sum_{i=1}^{2} \frac{L_{11}^{i} \cos^2 \theta_i + L_{22}^{i} \sin^2 \theta_i}{L_{11}^{i} L_{22}^{i}} \tag{22.b}$$

$$D_{12} = \sum_{i=1}^{2} \frac{\sin \theta_i \cos \theta_i (L_{11}^{i} - L_{22}^{i})}{L_{11}^{i} L_{22}^{i}} \tag{22.c}$$

$$W_{21} = \frac{(S_{12}^{*})^{i=2}}{L_{22}^{i=2}} - \frac{(S_{12}^{*})^{i=1}}{L_{22}^{i=1}} \tag{22.d}$$

In Eq. (22), superscripts 1 and 2 on L_{11}, L_{22} and S_{12} denote the upper and lower materials. Finally, explicit solution of matrix Λ are given by (Qian and Sun 1998)

$$\Lambda = \begin{bmatrix} (-iA\,\mathrm{sgn}(W_{21}) - D_{12})/\sqrt{2D_{11}}A & (-iA\,\mathrm{sgn}(W_{21}) - D_{12})/\sqrt{2D_{11}}A & 0 \\ \sqrt{D_{11}}/\sqrt{2}A & \sqrt{D_{11}}/\sqrt{2}A & 0 \\ 0 & 0 & 1/\sqrt{D_{33}} \end{bmatrix} \tag{23}$$

where

$$A = \sqrt{D_{11}D_{22} - D_{12}^2} \tag{24}$$

and sgn stands for sign function.

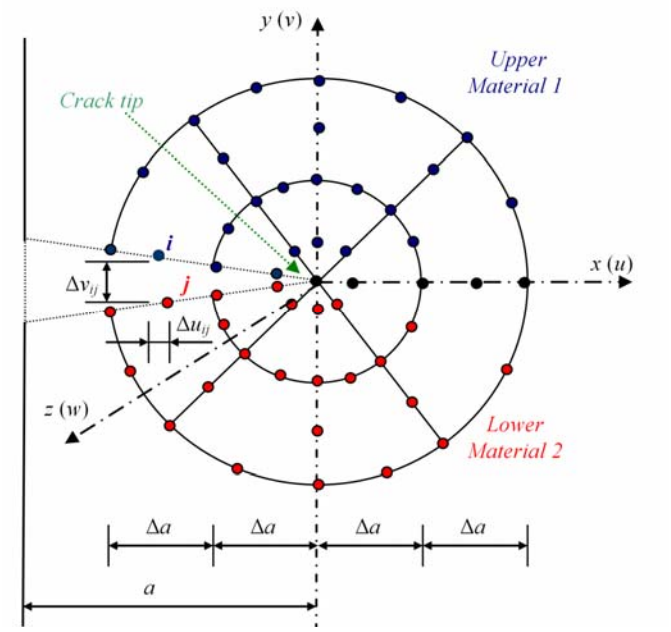

Fig. 2 Finite element model and calculation of relative crack displacements for the crack face

2.2 Numerical method

In order to calculate stress intensity factors, displacement extrapolation method is used. Displacement extrapolation method for interfacial crack between anisotropic materials can be written as (Nagai *et al*. 2007a, b)

$$\begin{Bmatrix} K_{II} \\ K_I \\ K_{III} \end{Bmatrix} = \lim_{r\to 0} \sqrt{\frac{\pi}{2r}} \Lambda \left\langle\!\left\langle \frac{(1+2i\varepsilon_\alpha)\cosh(\pi\varepsilon_\alpha)}{(r/l_k)^{i\varepsilon_\alpha}} \right\rangle\!\right\rangle \bar{\Lambda}^{-T} \begin{Bmatrix} \Delta u \\ \Delta v \\ \Delta w \end{Bmatrix} \tag{25}$$

where Δu, Δv, and Δw are relative crack surface displacements in the -x, -y, and -z directions, respectively.

In this study, the relative crack surface displacements Δu, Δv, and Δw across the crack faces are obtained from finite element method. For each coinciding nodes on crack surface near the crack tip, surface displacements are calculated and substituted into the Eq. (25) to obtain the stress intensity factor (Fig. 2). Then obtained stress intensity factors are plotted. Excluding the quarter point, a straight line is fit through the consecutive points near the crack tip and the correlation function R^2 is calculated. The line with R^2 closest to the unity is chosen provided it is sufficiently near the crack tip when $r \to 0$ (Sills *et al*. 2005).

2.3 Problem definition

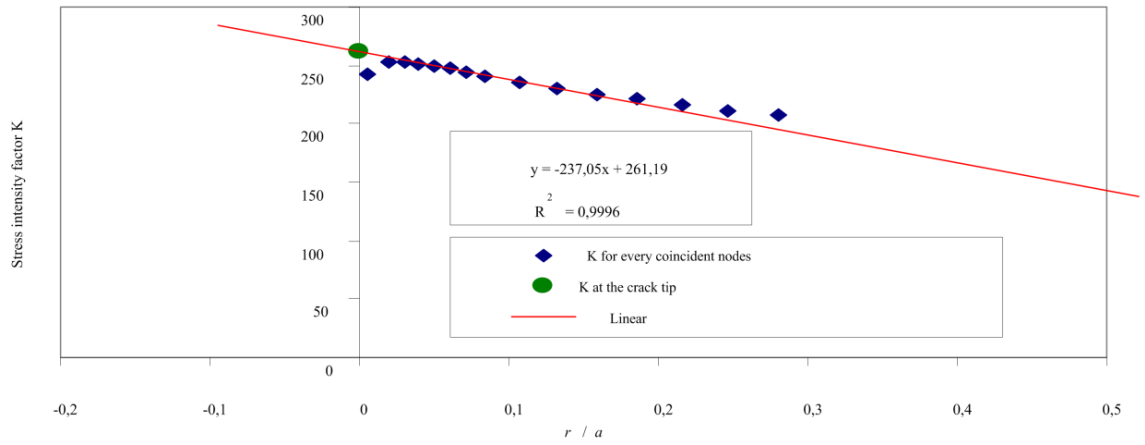

Fig. 3 Calculation of stress intensity factor at the crack tip according to the displacement extrapolation method

The dimensions of the specimen jointed with composite patch were chosen as 300 mm height, 50 mm-wide, and 2 mm-thick (Fig. 3). The interfacial crack length (a) between the composite plates was chosen to be 25 mm. A uniform tension stress (σ) of 50 MPa was applied on the upper edge, while it was fixed on the bottom edge of the plate. The single side of the composite plate was jointed from outside surface by using adhesive and carbon, boron, glass, or graphite composite patches. At the same time, these materials were selected as composite plate materials, too. The thickness (t_p) of the composite patches were chosen as 1.0 mm and the fiber orientation angles of the composite plates (θ_1 and θ_2) (Fig. 1) and the composite patch (θ_3) were varied from 0 to 90 degrees (Fig. 4). The material properties of the composites and the adhesive used in analyses are tabulated in Table 1. The Young's modulus, Poisson's ratio, and the thickness of the adhesive were taken as 1500 MPa, 0.3, and 0.3 mm, respectively.

Table 1 Material properties used in analyses

Material	E_1* (MPa)	E_2, E_3 (MPa)	G_{12}, G_{13} (MPa)	G_{23} (MPa)	ν_{12}, ν_{13} (-)	ν_{23} (-)
Boron/Epoxy	195120	25421	7234	4933	0.168	0.035
Graphite/Epoxy	172400	10340	4820	3100	0.3	0.18
Glass/Epoxy	27820	5830	2560	2240	0.31	0.41
Carbon/Epoxy	145000	10000	7000	3700	0.25	0.5
Adhesive	1500	1500	576.923	576.923	0.3	0.3

*E, G, and ν are Young modulus, Shear modulus, and Poisson's ratio, respectively
*1-Fiber longitudinal direction 2-Fiber transverse direction 3-Thickness direction

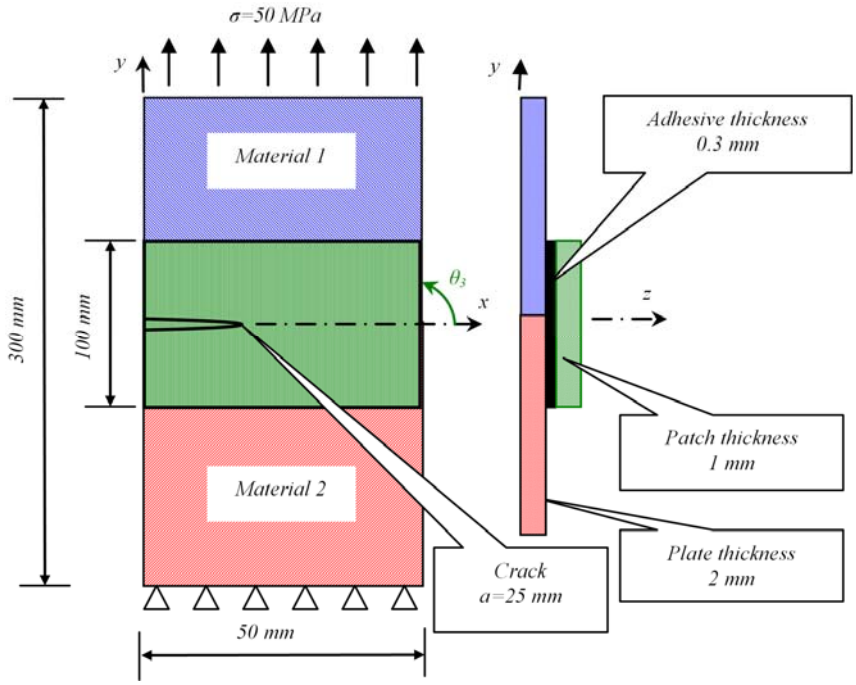

Fig. 4 Dimensions of the problem

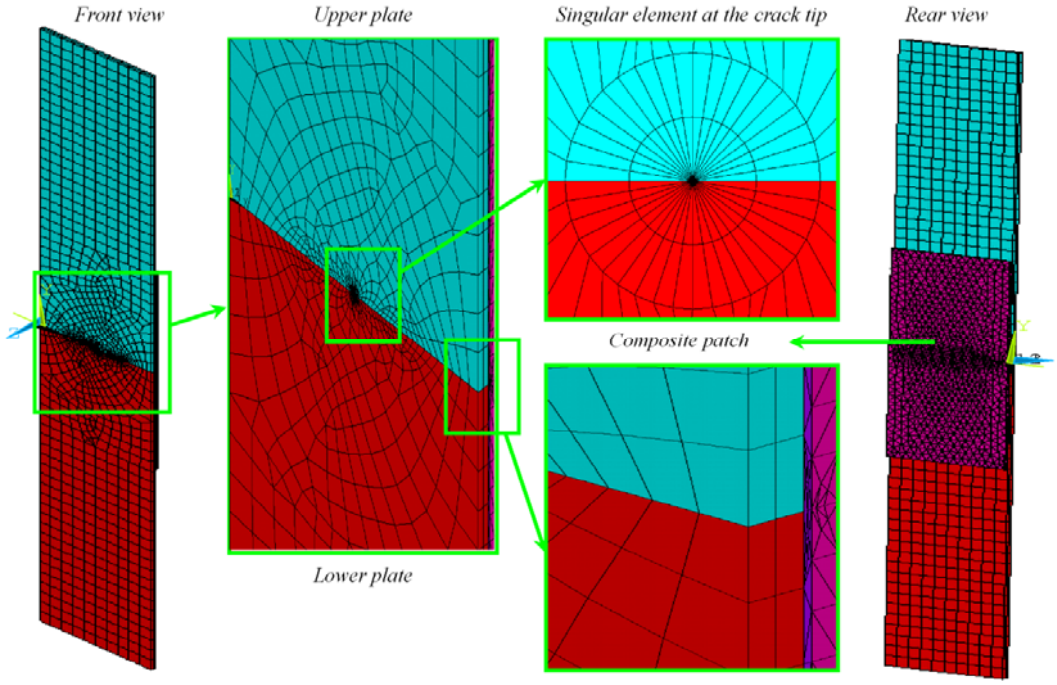

Fig. 5 Finite element model of the problem

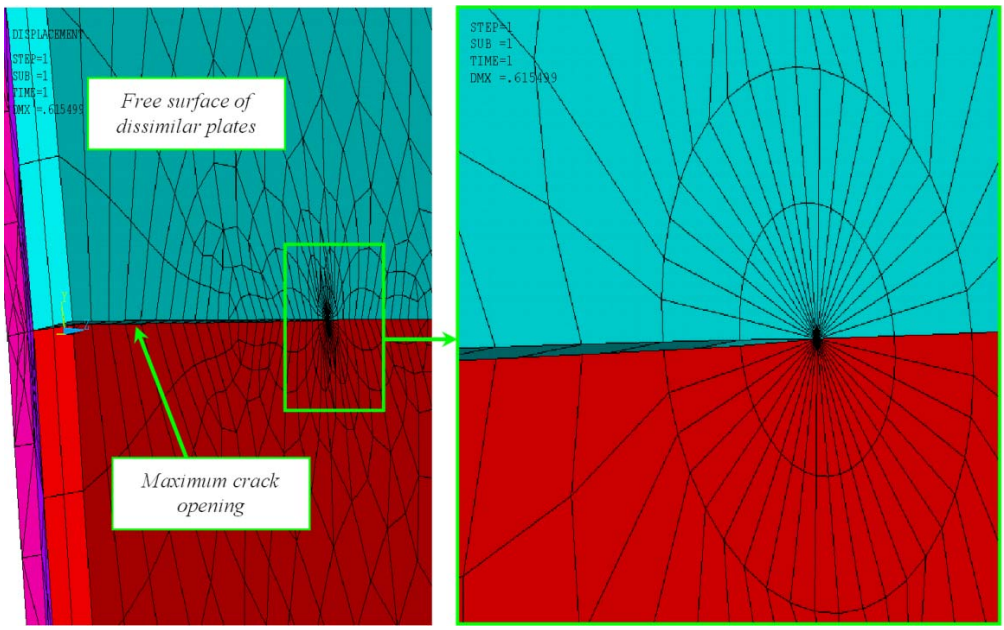

Fig. 6 Maximum crack opening at the free surface of two dissimilar orthotropic plates

Table 2 Material properties of two dissimilar orthotropic plates for centered crack problem

Mat.*	C_{11}	C_{12}	C_{13}	C_{22}	C_{23}	C_{33}	C_{44}	C_{55}	C_{66}
1	1.5958	0.3663	0.0197	0.8697	0.1591	0.8503	0.4132	0.2564	0.4274
2	2.8136	1.2582	0.8464	3.4895	0.8815	2.9452	1.0811	1.3298	1.3089

*Material No. 1: Aragonite; Material No. 2: Topaz

Table 3 Stress intensity factors for a 100m x 100m bimaterial plane strain problem

$[\theta_1 / \theta_2]$	$K_I / \sqrt{\pi a}$		$K_{II} / \sqrt{\pi a}$	
	Exact	Present study	Exact	Present study
[0 / 0]	1.0000	1.0018	0.1169	0.1146
[0 / 90]	1.0000	1.0011	0.1207	0.1210
[90 / 0]	1.0000	0.9965	0.0940	0.0983
[0 / -45]	1.0015	0.9970	0.1188	0.1160

2.4 The finite element model

The 3D finite element model of the problem is presented in Fig. 5. The 20-node *Solid95* type elements were used for the composite plates, the composite patch, and the adhesive, while,

singular element was used at the crack tip. The fiber orientation of the plate and the patch were obtained by modeling the coordinate system of elements with respect to θ_1, θ_2, and θ_3 (Okafor and Bhogapurapu 2006). Out of plane displacements and big local rotations occurred in 3D finite element model for the single side patch cases (Ayatollahi and Hashemi 2007, Madenci and Guven 2006, Turaga and Ripudaman 1999, Toudeshkya *et al*. 2011). Hence, to obtain more sensitive results, geometrically nonlinear analyses were carried out in this study. The maximum crack opening was obtained in the free surface of the repaired composite plate (Fig. 6). For this reason, the SIF values were calculated from the displacements (obtained with FEA by using *ANSYS* software) at the free surface of the composite plate (ANSYS 2009).

3. Results and discussion

First of all, for the verification of the analysis procedure, an unrepaired plate with a crack example that exists in the literature was modeled in this study (Fig. 7). The unrepaired plate model consisted of 17195 nodes and 5800 *Plane82* elements. The material properties were given in Table 2. The normalized values ($K_I / \sqrt{\pi a}$) of the calculated SIF values are presented in Table 3.

The variation of the SIF (K_I) with respect to the fiber orientation angle (θ_1) of the upper plate for different fiber orientation angle (θ_3) of the composite patch is presented in Fig. 8. For all values of θ_1, the K_I decreased with the increase of fiber orientation angle of the composite patch. The load carried by fibers increased with the increase in θ_3, so that the strength of the plate. The increase in θ_1 increased the K_I for all values of θ_3. However, the increase in K_I was larger for larger values of θ_3. The change in the K_I from $\theta_1 = 0°$ to 90° was 31.95 $MPa\sqrt{mm}$ for $\theta_3 = 0°$, while it was 52.72 $MPa\sqrt{mm}$ for $\theta_3 = 90°$. Also, it was observed that the increase in θ_1 did not change the effect of the patch's fiber orientation angle on the K_I. The change in the K_I from $\theta_3 = 0°$ to 90° was

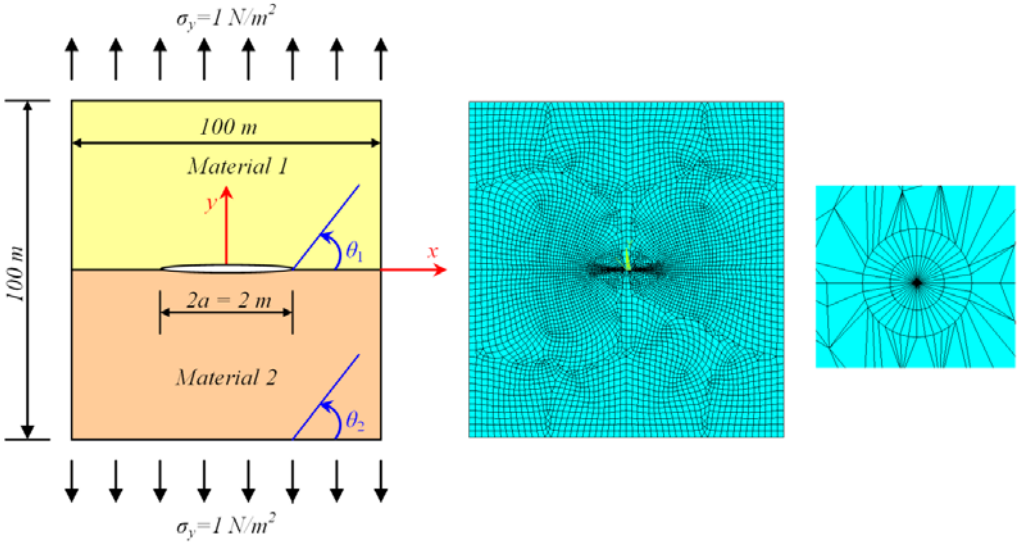

Fig. 7 Interfacial centered crack problem

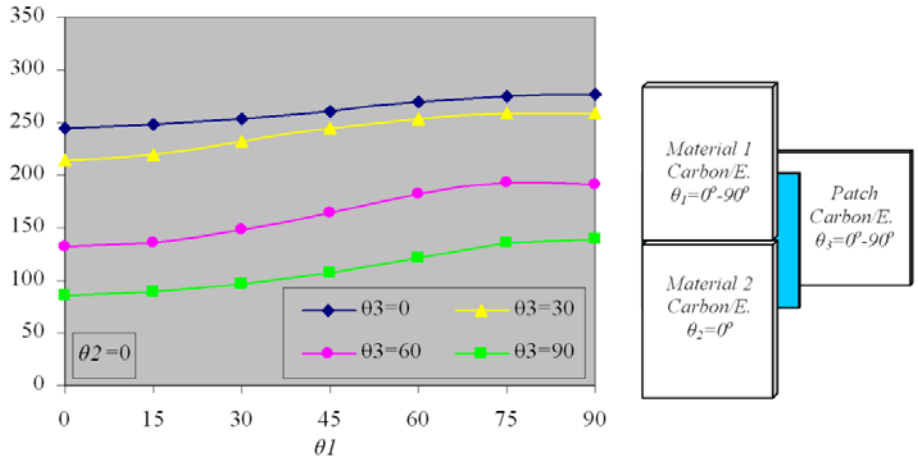

Fig. 8 Variation of K_I (MPa $\sqrt{mm}$) with the θ_1 for different composite patch angles θ_3 when $\theta_2 = 0$

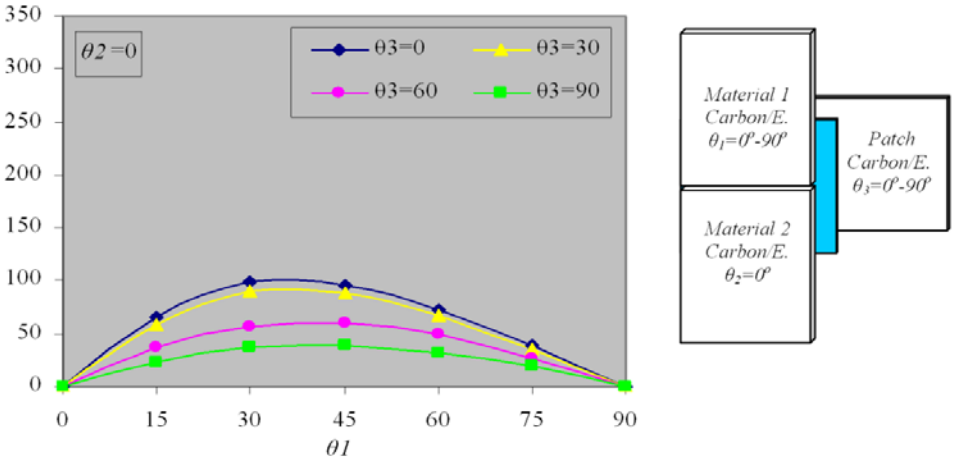

Fig. 9 Variation of K_{II} (MPa $\sqrt{mm}$) with the θ_1 for different composite patch angles θ_3 when $\theta_2 = 0$

158.26 $MPa\sqrt{mm}$ for $\theta_1 = 0°$, while it was 137.49 $MPa\sqrt{mm}$ for $\theta_1 = 90°$.

The values of the K_{II} were smaller when compared to K_I. K_{II} decreased with the increase of composite patch's fiber orientation angle, except for $\theta_1 = 0°$ and 90° (Fig. 9). The maximum value of the K_{II} was calculated as 98.29 $MPa\sqrt{mm}$ for $\theta_3 = 0°$.

While investigating the effect of varying fiber orientation angle θ_1 for different composite patch materials (carbon/epoxy, boron/epoxy, graphite/epoxy, and glass/epoxy), the fiber orientation angle of lower plate and the composite patch were chosen to be constant ($\theta_2 = \theta_3 = 0$) (Fig. 10). Among the all patch material types, the boron/epoxy had the highest values of E_1 and E_2, while the glass/epoxy had the lowest values. Hence, the maximum value (K_I) was calculated as 320.25

$MPa\sqrt{mm}$ for glass/epoxy composite patch at $\theta_1 = 90°$ and the minimum was calculated as 167.38 $MPa\sqrt{mm}$ for boron/epoxy composite patch at $\theta_1 = 0°$. Since the mechanical characteristics of the carbon/epoxy and graphite/epoxy are almost same, the variation of SIF with respect to the θ_1 was obtained on top of each other for these composite patch materials. The increase of θ_1 increased the value of K_I for each material. However, the increase in the value of K_I was smaller for stronger composite patch material, such as boron/epoxy. The change in the value of K_I from $\theta = 0°$ to 90° for boron/epoxy was 21.91 $MPa\sqrt{mm}$, while it was 49.17 $MPa\sqrt{mm}$ for glass/epoxy material.

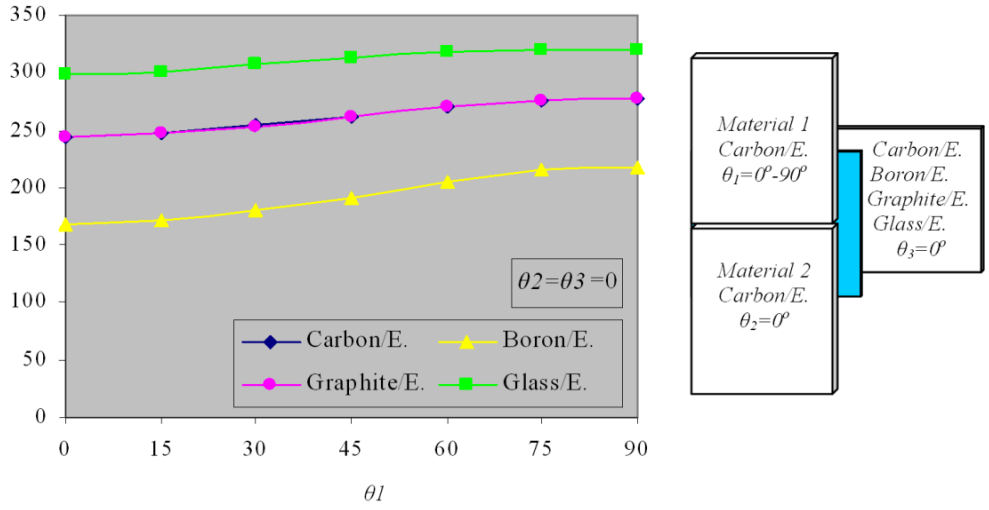

Fig. 10 Variation of K_I (MPa $\sqrt{mm}$) with the θ_1 for different composite patch materials when $\theta_2 = \theta_3 = 0$

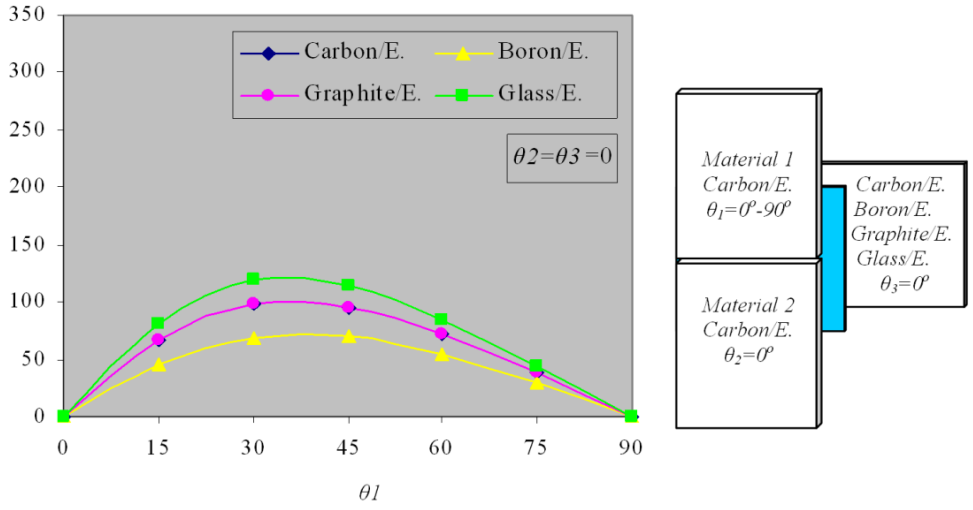

Fig. 11 Variation of K_{II} (MPa $\sqrt{mm}$) with the θ_1 for different composite patch materials when $\theta_2 = \theta_3 = 0$

K_{II}, which was observed mostly for mixed mode loading conditions (for θ_1 values different than 0° and 90°), had smaller values when compared to K_I. As it was observed for K_I, the values of K_{II} increased with use of softer composite patch material (Fig. 11). The maximum value of K_{II} was calculated as 320.25 $MPa\sqrt{mm}$ for glass/epoxy composite patch material at $\theta_1 = 30°$. The value of K_{II} was increased with the increase of θ_1 up to 30° for carbon/epoxy, graphite/epoxy, and glass/epoxy composite patch materials then decreased to zero with the increase of θ_1 up to 90°. For boron/epoxy composite patch material the behavior was same but the increase continued until θ_1 reached to 45°.

The effect of the fiber orientation angle (θ_1) for different lower plate materials (boron/epoxy, graphite/epoxy, and glass/epoxy) on the stress intensity factor (K_I and K_{II}) is presented in Fig. 12. The fiber orientation angle of lower plate and the composite patch were chosen to be constant ($\theta_2 = \theta_3 = 0$). The increase of θ_1 increased the value of K_I for each material type. However, the increase in the value of K_I was larger for stronger lower plate material, such as boron/epoxy. The use of stronger lower plate material resulted with an increase also in the values of K_{II} (Fig. 12). The value of K_{II} was increased with the increase of θ_1 up to 45° for boron/epoxy and graphite/epoxy lower plate materials then decreased to zero with the increase of θ_1 up to 90°. For glass/epoxy lower plate the behavior was same but the increase continued until θ_1 reached to 60°.

The investigation of the patching two different materials (boron/epoxy, graphite/epoxy, and glass/epoxy were used as lower plate, while the carbon/epoxy, boron/epoxy, graphite/epoxy, and glass/epoxy were used as upper plate) that have the same fiber orientation angle ($\theta_1 = \theta_2$) presented that the value of the K_I increases as the fiber orientation angle ($\theta_1 = \theta_2$) increased (Fig. 13). However, the increase in the value of K_I was larger for stronger plate material combinations, such as carbon-boron (C-B in the Fig. 13). Since the material characteristics of Carbon and Boron are similar, a similar behavior was observed in case of Carbon-Graphite and Boron-Graphite plate material combinations. The use of softer lower plate in plate material combinations was resulted

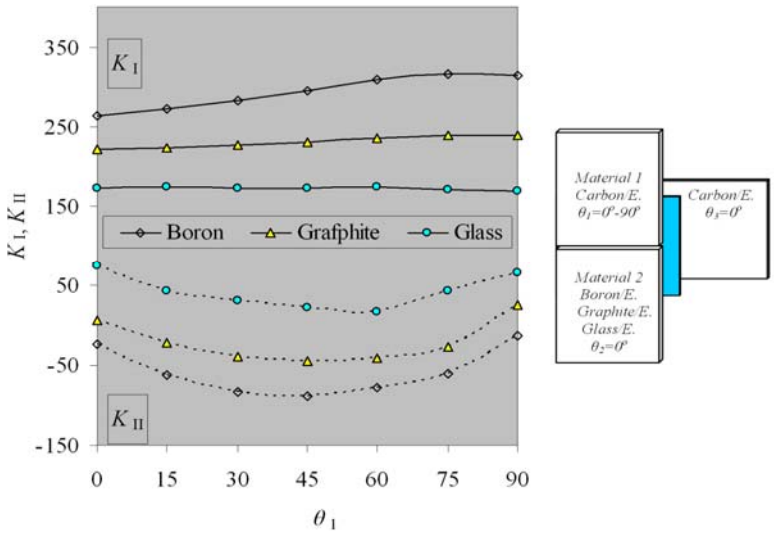

Fig. 12 Variation of K_I and K_{II} (MPa $\sqrt{mm}$) with the θ_1 for different lower materials when $\theta_2 = \theta_3 = 0$

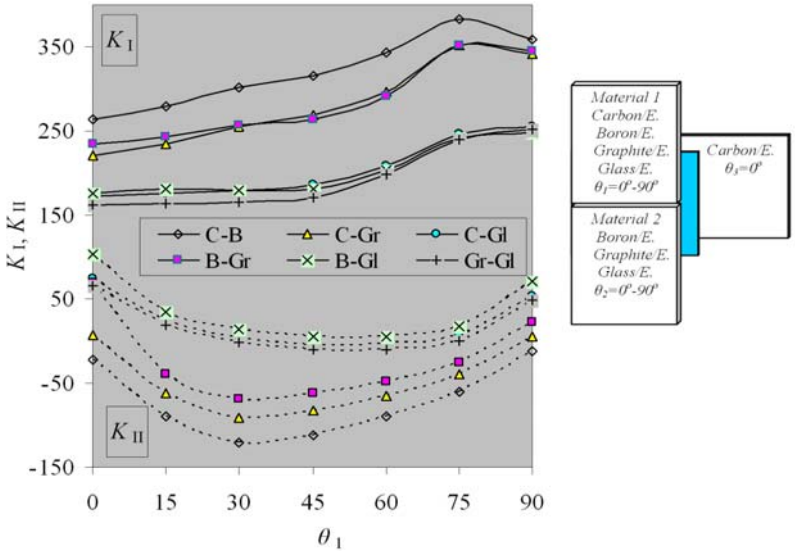

Fig. 13 Variation of K_I and K_{II} (MPa$\sqrt{mm}$) with the $\theta_1 = \theta_2$ for different lower and upper materials when $\theta_3 = 0$

with approximately same behavior regardless the type of the upper plate.

Similar behaviors were observed for the variation of K_{II} with respect to the material combinations and fiber orientation angles (Fig. 13). The value of K_{II} was increased with the increase of θ_1 up to 30° for carbon-boron, carbon-graphite, and boron-graphite plate materials then decreased to zero with the increase of θ_1 up to 90°. For the use of glass/epoxy lower plate in a combination with carbon/epoxy, boron/epoxy, and graphite/epoxy upper plate the behavior was same but the increase continued until θ_1 reached to 60°.

4. Conclusions

The interfacial edge crack problem on dissimilar orthotropic plates that are jointed with adhesive and repaired with composite patch at single side were numerically analyzed by using displacement extrapolation method in this study. The displacements of the nodes at crack surface were calculated by using a 3D finite element model in ANSYS FEA software. The fiber orientation angle of orthotropic composite plates and composite patches were varied. The results of stress intensity factor that were obtained for various composite material configurations can be summarized as follows:

- Increasing the fiber orientation angle of upper plate (θ_1) increases the stress intensity factor – K_I.
- The increase in fiber orientation angle of composite patch (θ_3) decreases the stress intensity factor – K_I. Increasing the θ_1 does not change the effect of fiber orientation angle of composite patch on K_I.
- K_{II} has smaller values when compared to K_I. Except for θ_1 = 0° and 90°, K_{II} decreases with

an increase in composite patch's fiber orientation angle.
- The variation of the K_I at all values of θ_1 with respect to the material type is boron/epoxy > carbon/epoxy = graphite/epoxy > glass/epoxy.
- Both the values of K_I and K_{II} increase as the material becomes softer.

To conclude, the use of the composite patch has an important role in the repair of interface cracks. The choose of fiber orientation angle in the direction of the load to be carried will considerably decrease the stress intensity factor, hence will prevent the opening of the crack. Besides the fiber orientation angle of the composite patch, the material type of the patch has an importance in repair applications. It is important to choose a patch material type that has higher modulus elasticity (in the loading direction) than the plates to be repaired. In application, to obtain an efficient repair of the interface crack, these can be listed as the primary recommendations.

References

Abdelaziz, A.T., Boukhili, R., Achiou, S., Gordon, S. and Boukheli, H. (2006), "Bonded joints with composite adherents. Part I. effect of specimen configuration, adhesive thickness, spew filet and adherent stiffness on fracture", *Int. J. Adhes. Adhes.*, **26**, 226-236.

Albedah, A., Bouiadjra, B.B., Mhamdia, R., Benyahia, F. and Es-Saheb, M. (2011), "Comparison between double and single sided bonded composite repair with circular shape", *Mater. Des.*, **32**(2), 996-1000.

ANSYS (2009), *Academic Teaching Introductory Help Menu*.

Apalak, Z.G. (2006), "Progressive damage modeling of an adhesively bonded unidirectional composite single – lap joint in tension at the meso scale level", *J. Thermoplast Compos. Mater.*, **19**(6), 671-702.

Atas, C., Akgun, Y., Dagdelen, O., Icten, B.M. and Sarikanat, M. (2011), "An experimental investigation on the low velocity impact response of composite plates repaired by VARIM and hand lay-up processes", *Compos. Struct.*, **93**(3), 1178-1186.

Ayatollahi, M.R. and Hashemi, R. (2007), "Mixed mode fracture in an inclined center crack repaired by composite patching", *Compos. Struct.*, **81**, 264–273

Barnett, D.M. and Lothe, J. (1973), "Synthesis of the sextic and the integral formalism for dislocations, greens function and surface waves in anisotropic elastic solids", *Physica Norvegica*, **7**, 13-9.

Belhouari, M., Bouiadjra, B.B., Megueni, A. and Kaddouri, K. (2004), "Comparison of double and single bonded repairs to symmetric composite structures: A numerical analysis", *Compos. Struct.*, **65**(1), 47-53.

Bezzerrouki, M., Bouiadjra, B.B. and Ouinas, D. (2008), "SIF for cracks repaired with single composite patch having two adhesive bands and double symmetric one in aircraft structures", *Int. J. Comput. Mater. Sci. Surf. Eng.*, **44**(2), 542-546.

Bouiadjra, B.B., Fekirini, H., Serier, B. and Benguediab, M. (2007), "Numerical analysis of the beneficial effect of the double symmetric patch repair compared to single one in aircraft structures", *Int. J. Comput. Mater. Sci. Surf. Eng.*, **38**(4), 824-829.

Dongye, C. and Ting, T.C.T. (1989), "Explicit expressions of Barnett Lothe tensors and their associated tensors for orthotropic materials", *Q. Appl. Math.*, **47**, 732-734.

Gu, L., Kasavajhala, A.R.M. and Zhao, S. (2011), "Finite element analysis of cracks in aging aircraft structures with bonded composite-patch repairs", *Composites Part B*, **42**(3), 505-510.

Hemanth, D., Aradhya, S.K.S., Murthy, R.T.S. and Raju, N.G. (2005), "Strain energy release rates for an interface crack in orthotropic media—a finite element investigation", *Eng. Fract. Mech.*, **72**(5), 759-772.

Her, S.C. (1999), "Stress analysis of adhesively bonded-lap joints", *Compos. Struct.*, **47**(1-4), 673-678.

Hwu, C. (1993), "Explicit solutions for collinear interface crack problems", *Int. J. Solids Struct.*, **30**(3), 301-312.

Ikeda, T., Nagai, M., Yamanaga, K. and Miyazaki, N. (2006), "Stress intensity factor analyses of interface cracks between dissimilar anisotropic materials using the finite element method", *Eng. Fract. Mech.*,

73(14), 2067-2079.
Jones, R. and Chiu, W.K. (1999), "Composite repairs to cracks in thick metallic components", *Compos. Struct.*, **44**(1), 17-29.
Liou, J.Y. and Sung, J.C. (2008), "On the Barnett–Lothe tensors for anisotropic elastic materials", *Eur. J. Mech. A Solids*, **27**(6), 1140-1160.
Madani, K., Touzain, S., Feaugas, X., Benguediab, M. and Ratwani, M. (2008), "Numerical analysis for the determination of the stress intensity factors and crack opening displacements in plates repaired with single and double composite patches", *Int. J. Comput. Mater. Sci. Surf. Eng.*, **42**(3), 385-393.
Madenci, E. and Guven, I. (2006), *The Finite Element Method and Applications in Engineering Using ANSYS*, Springer, New York
Nagai, M., Ikeda, T. and Miyazaki, N. (2007a), "Stress intensity factor analysis of an interface crack between dissimilar anisotropic materials under thermal stress using the finite element analysis", *Int. J. Fract.*, **146**(4), 233-248.
Nagai, M., Ikeda, T. and Miyazaki, N. (2007b), "Stress intensity factor analysis of a three-dimensional interface crack between dissimilar anisotropic materials", *Eng. Fract. Mech.*, **74**(16), 2481-2497.
Okafor, A.C. and Bhogapurapu, H. (2006), "Design and analysis of adhesively bonded thick composite patch repair of corrosion grind-out and cracks on 2024 T3 clad aluminum aging aircraft structures", *Compos. Struct.*, **76**(1-2), 138-150.
Oudad, W., Bouiadjra, B.B., Belhouari, M., Touzain, S. and Feaugas, X. (2009), "Analysis of the plastic zone size ahead of repaired cracks with bonded composite patch of metallic aircraft structures", *Int. J. Comput. Mater. Sci. Surf. Eng.*, **46**(4), 950-954.
Qian, W. and Sun, C.T. (1998), "Methods for calculating stress intensity factors for interfacial cracks between two orthotropic solids", *Int. J. Solids Struct.*, **35**(25), 3317-3330.
Rogel, L. and Sills, L.B. (2010), "A through interface crack between a transversely isotropic pair of materials (+30°/−60°, −30°/+60°)", *Eng. Fract. Mech.*, **77**(16), 3261-3291.
Schubbe, J.J. and Mall, S. (1999), "Investigation of a cracked thick aluminum panel repaired with a bonded composite patch", *Eng. Fract. Mech.*, **63**(3), 305-323.
Seo, D.C. and Lee, J.J. (2002), "Fatigue crack growth behavior of cracked aluminum plate repaired with composite patch", *Compos. Struct.*, **57**(1-4), 323-330.
Sheppard, A., Kelly, D. and Tong, L. (1998), "A damage zone model for the failure analysis of adhesively bonded joints", *Int. J. Adhes. Adhes.*, **18**(6), 385-400.
Sills, L.B., Hershkovitz, I., Wawrzynek, P.A., Eliasi, R. and Ingraffea, A.R. (2005), "Methods for calculating stress intensity factors in anisotropic materials: part I—$z = 0$ is a symmetric plane", *Eng. Fract. Mech.*, **72**(15), 2328-2358.
Sills, L.B. and Ikeda, T. (2011), "Stress intensity factors for interface cracks between orthotropic and monoclinic material", *Int. J. Fract.*, **167**(1), 47-56.
Stroh, A.N. (1962), "Steady state problems in anisotropic elasticity", *J. Math. Phys.*, **41**(2), 77-103.
Sun, C.T. and Qian, W. (1997), "The use of finite extension strain energy release rates in fracture of interfacial cracks", *Int. J. Solids Struct.*, **34**(20), 2595-2609.
Temiz, S. (2006), "Application of bi-adhesive in double-strap joints subjected to bending moment", *J. Adhes. Sci. Technol.*, **20**(14), 1547-1560.
Ting, T.C.T. (1986), "Explicit solution and invariance of the singularities at an interface crack in anisotropic composites", *Int. J. Solids Struct.*, **22**(9), 965-983.
Toudeshkya, H.H., Ghaffaria, M.A. and Mohammadib, B. (2011), "Fatigue propagation of induced cracks by stiffeners in repaired panels with composite patches", *Pro. Eng.*, **10**, 3285-3290.
Turaga, V.R.S. and Ripudaman, S. (1999), "Modeling of patch repairs to a thin cracked sheet", *Eng. Fract. Mech.*, **62**(2-3), 267-289.
Zhang, Y., Vassilopoulos, A.P. and Keller, T. (2010), "Effects of low and high temperatures on tensile behavior of adhesively-bonded GFRP joints", *Compos. Struct.*, **92**(7), 1631-1639.

CC